Published in final edited form as:
Photochem Photobiol Sci. 2010 November ; 9(11): 1480–1489. doi:10.1039/c0pp00207k.

Fundus autofluorescence and the bisretinoids of retina†

Janet R. Sparrow[*,a,b], **Yalin Wu**[a], **Takayuki Nagasaki**[a], **Kee Dong Yoon**[a], **Kazunori Yamamoto**[a], and **Jilin Zhou**[a]

[a]Department of Ophthalmology, Columbia University, 630 W. 168th Street, New York, NY, 10032, USA

[b]Department of Pathology and Cell Biology, Columbia University, 630 W. 168th Street, New York, NY, 10032, USA

Abstract

Imaging of the human fundus of the eye with excitation wavelengths in the visible spectrum reveals a natural autofluorescence, that in a healthy retina originates primarily from the bisretinoids that constitute the lipofuscin of retinal pigment epithelial (RPE) cells. Since the intensity and distribution of fundus autofluorescence is altered in the presence of retinal disease, we have examined the fluorescence properties of the retinal bisretinoids with a view to aiding clinical interpretations. As is also observed for fundus autofluorescence, fluorescence emission from RPE lipofuscin was generated with a wide range of exciting wavelengths; with increasing excitation wavelength, the emission maximum shifted towards longer wavelengths and spectral width was decreased. These features are consistent with fluorescence generation from a mixture of compounds. While the bisretinoids that constitute RPE lipofuscin all fluoresced with maxima that were centered around 600 nm, fluorescence intensities varied when excited at 488 nm, the excitation wavelength utilized for fundus autofuorescence imaging. For instance the fluorescence efficiency of the bisretinoid A2-dihydropyridine-phosphatidylethanolamine (A2-DHP-PE) was greater than A2E and relative to both of the latter, all-*trans*-retinal dimer-phosphatidylethanolamine was weakly fluorescent. On the other hand, certain photooxidized forms of the bisretinoids present in both RPE and photoreceptor cells were more strongly fluorescent than the parent compound. We also sought to evaluate whether diffuse puncta of autofluorescence observed in some retinal disorders of monogenic origin are attributable to retinoid accumulation. However, two retinoids of the visual cycle, all-*trans*-retinyl ester and all-*trans*-retinal, did not exhibit fluorescence at 488 nm excitation.

Introduction

The retina of the eye exhibits an inherent autofluorescence that is imaged clinically by ophthalmoscopy[1,2] and that has been studied by noninvasive spectrofluorometry[3] and adaptive optics.[4] The spectral features, spatial distribution, age-dependent intensities and disease-related characteristics of fundus autofluorescence indicate that this emission derives

†This article is published as part of a themed issue on photosensitive visual pigments: opsins and retinoids.

*jrs88@columbia.edu; Fax: +1 212-305-9638; Tel: +1 212-305-9944 .

from the complex mixture of bisretinoid pigments that accumulate in retinal pigment epithelial (RPE) cells as lipofuscin.[5,6] The extensive system of conjugated double bonds within these retinoid-derived fluorophores also explains the long wavelength fluorescence emission of RPE lipofuscin.

The autofluorescence of the fundus is typically excited by wavelengths ranging from approximately 488 nm, the excitation employed with a confocal scanning laser ophthalmoscope (cSLO) to 550 nm.[5,6] The fluorescence emission of fundus autofluorescence measured spectrophotometrically is broad and centered at approximately 610 nm.[5,7] The lipofuscin-related pigments of retina that have been identified thus far exhibit various absorbance maxima in the visible spectrum including 430 nm (all-*trans*-retinal dimer), 439 nm (A2E), 449 nm (A2PE), 426 nm (isoA2E), 490 nm (A2-dihydropyridine-phosphatidylethanolamine, A2-DHP-PE) and 510 nm (all-*trans*-retinal dimer-phosphatidylethanolamine and all-*trans*-retinal dimer-ethanolamine).[8-11]

The lipofuscin of RPE cells is unique: the bisretinoids that constitute this material form as a consequence of the light capturing function of the retina. Thus when the 11-*cis*- and all-*trans*-retinal chromophores of visual pigment are absent, such as in patients with early-onset retinal dystrophy associated with mutations in RPE65,[12] RPE lipofuscin does not form and fundus autofluorescence is absent.[12] On the other hand, abundant accumulations of RPE bisretinoids give rise to elevated fundus autofluorescence in retinal disorders such as recessive Stargardt disease,[13-17] dominant Stargardt-like macular degeneration,[18] and in Best vitelliform macular dystrophy.[6,19] The bisretinoids of RPE lipofuscin are also implicated in disease processes associated with age-related macular degeneration (AMD).[20-23]

In addition to generalized changes in fundus autofluorescence intensity, abnormal patterning of autofluorescence is a feature of some retinal disorders. For instance, regions of reduced or absent fundus autofluorescence can be indicative of RPE cell atrophy or death.[24,25] Localized areas of enhanced fundus autofluorescence are also often observed, most notably the elevated signals at the margin of geographic atrophy[24,26] and the intense autofluorescence observed within the parafoveal rings in some patients with retinitis pigmentosa.[25]

Here we examine features of the lipofuscin fluorophores of retina that are significant to the interpretation of fundus autofluorescence.

Experimental

Tissue

A human eye (age 52 years) was obtained from a donor through the National Disease Research Interchange (Philadelphia, PA, USA).

Reagents and compound synthesis

All-*trans*-retinal, ethanolamine, trifluoroacetic acid (TFA), dipalmitoyl-phosphatidylethanolamine (DP-PE), retinyl palmitate and formic acid were purchased from

Sigma-Aldrich (St. Louis, MO, USA); acetonitrile was purchased from Fisher (Fair Lawn, NJ, USA) and PBS (Dulbecco's phosphate buffered saline) was from Invitrogen (Carlsbad, CA, USA). All other chemicals were obtained from Sigma-Aldrich. A2E was synthesized from all-*trans*-retinal and ethanolamine[8] and A2PE (DP-A2PE) was generated by reaction of all-*trans*-retinal and dipalmitoyl-phosphatidylethanolamine (DP-PE).[27] All-*trans*-retinal dimer was synthesized as formerly published,[9] as was A2-DHP-PE.[11] The structures of synthesized standards of these compounds have been corroborated.[8,9,11,27-29] Photooxidized-A2E was obtained by irradiating (430 ± 20 nm, 1.3 mW cm^{-2}) A2E (100-200 μM in PBS with 1% DMSO) for the durations indicated.

Spectroscopy

Spectra in solvents were obtained at room temperature using a FluoroMax 4 spectrofluorometer (Horiba Scientific, USA), quartz cuvettes (Helma; Fisher Scientific) and 10 mm light path. Bandpass slit was set at 6-10 nm as indicated. Spectral width was measured as the wavelength at which intensity was half maximal. With repeated excitation (×10) of a single sample of retinoid or bisretinoid, the emission profile did not change; this observation indicated that the samples were not subject to photo-oxidation under the conditions utilized for spectroscopy.

Spectra from the lipofuscin in human RPE cells were obtained using cryostat sections and a fluorescence microscope (Zeiss Axioskop2) equipped with a CCD camera (Orca 100, Hamamatsu, Japan) and a Varispec liquid crystal tunable filter (Cambridge Research & Instrumentation, Woburn, MA, USA), all of which were controlled by Metamorph (Molecular Devices, Downingtown, PA, USA). The following filter sets (Chroma Technology Corp., Bellows Falls, VT, USA) were used (wavelengths of excitation, dichroic and barrier filter in nm): UV (330 ± 40, 400, >400); cyan (436 ± 10, 455, >460), blue (480 ± 20, 505, >510), red (545 ± 15, 565, >572). An average spectrum of five areas (3.3 μm diameter circle) was obtained after subtracting background areas within the image using ImageJ (http://rsb.info.nih.gov/ij/).

HPLC and UPLC-MS

Compound elution was achieved using an Alliance HPLC (Waters Corp Milford, MA, USA) with a Delta Pak*[circlecopyrt]*R C4 (5 μm, 3.9 × 150 mm; Waters) or an Atlantis*[circlecopyrt]*R dC18 (3 μm, 4.6 × 150 mm; Waters) column. The mobile phase for the C4 column a gradient of acetonitrile in water with 0.1% trifluoroacetic acid: 0-5 min; 75% acetonitrile, flow rate, 0.8 ml min^{-1}; 5-30 min, 75-100% acetonitrile; flow rate, 0.8 ml min^{-1}; 30-35 min, 100% acetonitrile, flow rate, 0.8-1.2 ml min^{-1}; 35-50 min, 100% acetonitrile, flow rate, 1.2 ml min^{-1}. With the dC18 column a gradient of acetonitrile in water with 0.1% trifluoroacetic acid was utilized: 75-90% acetonitrile (0-30 min); 90-100% acetonitrile (30-40 min); 100% acetonitrile (40-100 min) with a flow rate of 0.5 ml min^{-1}. Absorbance (Waters 2996 Photodiode Array) and fluorescence (Water 2475 Multi λ Fluorescence Detector; 18 nm bandwidth) were detected at wavelengths indicated. Fluorescence efficiency was estimated as fluorescence peak area (μV s)/absorbance peak area (μV s).

UPLC-MS analysis was performed on a Waters Acquity UPLC system (Waters, New Jersey, USA) that was coupled on-line with a Waters SQD single quadrupole mass spectrometer and both PDA eλ and fluorescence (FLR, Waters) detectors. The mass spectrometer was equipped with ESCi (electrospray ion multimode ionization) and ion trap analyzer operating in full scan mode from mass to charge ratio (*m*/*z*) 200-1200. For compound elution, an Xbridge[*circlecopyrt*]R C18 column (2.5 μm, 3.0 × 50 mm I.D.) was used for the stationary phase and for the mobile phase a linear gradient (65-90%) of a 1: 1 mixture of acetonitrile and methanol (0-25 min) with 0.1% formic acid and a flow rate of 0.5 ml min^{-1}.

Results and discussion

The emission maximum of RPE lipofuscin undergoes excitation-dependent shifts

Emission spectra of RPE lipofuscin measured from histological sections of human retina were readily obtained with a broad range of excitation wavelengths (330-545 nm) (Fig. 1). The spectra varied according to the excitation wavelength utilized (330, 436, 480, 545 nm) with excitation at progressively longer wavelengths resulting in spectra that were reduced in width. Specifically, spectral width was ~190 nm with excitation at 330 nm and was ~60 nm with excitation at 545 nm. This observation likely indicates that with excitation at shorter wavelengths, fluorescence arisesfrom a mixture of components (including photooxidized forms of bisretinoid and bisretinoid photocleavage products) with varying emission maxima, while with excitation at longer wavelengths, emission is generated from fewer compounds. The transition from 436 to 545 nm excitation was also associated with a shift in emission maximum toward longer wavelengths (from 590 to 630 nm) (Fig. 1). A similar red-shift in fundus autofluorescence is observed as the excitation wavelength is increased.[30] Overall, these spectral characteristics are consistent with fluorescence emission from a complex blend of compounds.

Bisretinoids exhibit fluorescence of different intensities

The fluorescence emission of the bisretinoid pigments of retina is generally maximal at approximately 600-620 nm. With excitation at 488 nm, the wavelength typically utilized for fundus autofluorescence imaging, we found that the emission maximum of A2E was solvent-dependent: 612 nm in methanol and blue-shifted (to 605 nm) in the more hydrophobic solvent, chloroform (Fig. 2A, B). The emission maximum of A2E in PBS with 2% DMSO was similar (604 nm) to that in chloroform (605 nm) (Fig. 2C). The foregoing solvent-dependency is consistent with our previous findings.[31] In both methanol and chloroform, but not in PBS/DMSO, there was also a red-shift in emission maxima as the excitation wavelength was increased from 430-488 nm (Fig. 2A, B). The bisretinoid all-*trans*-retinal dimer exhibited even greater solvent-related variability, with emission maxima at 540 and 570 nm (λ_{ex} 430 nm) for chloroform and methanol respectively, and a maxima at 610 nm for PBS/DMSO (λ_{ex} 430 nm and 488) (Fig. 3A, B). For another bisretinoid, A2-DHP-PE, the emission maximum was 610 nm (λ_{ex} 488) in methanol (Fig. 3C).

The contributions that individual bisretinoids make to fundus autofluorescence can be influenced not only by their excitation and fluorescence spectra but also by their abundance and fluorescence efficiency. Indeed the various bisretinoids exhibit fluorescence intensities

that are different. For instance, at an excitation of 488 nm, the wavelength generally utilized for fundus autofluorescence imaging, the fluorescence exhibited by A2-DHP-PE (λ_{max} ~ 337, 490) relative to absorbance was of greater efficiency than A2E and isoA2E (Fig. 4) (fluorescence efficiencies: A2E, 4074; isoA2E, 24422; A2-DHP-PE, 385,869). On the other hand, all-*trans*-retinal dimer-phosphatidylethanolamine (all-*trans*-retinal dimer-PE) isweakly fluorescent (Fig. 4); this finding is consistent with our previous results.[32]

Altered fluorescence efficiency and hypsochromic shifts in fluorescence associated with photooxidation

One can expect the excitation and emission spectra of fundus autofluorescence to be determined by the fluorescence properties of the various lipofuscin constituents and their relative abundance. In addition, however, photooxidation of the bisretinoids of lipofuscin can also change their fluorescence intensities.[32,33] Shown in Fig. 5 is the chromatographic detection of A2E, isoA2E and oxidized forms of A2E with online monitoring of fluorescence, UV-visible absorbance and mass (*m*/*z*). The starting sample of A2E/isoA2E was photooxidized by exposure to 430 nm light. On the C18 column, all of the photooxidized forms of A2E (Fig. 5: peaks 1, 2, 3) exhibit shorter retention times than A2E (Fig. 5: peak 4) because of increased polarity. The fluorescence intensities of some photooxidized forms of A2E are greater than A2E. Specifically, photooxidation at one carbon-carbon double bond along the short-arm of A2E (Fig. 5: peaks 1 and 3) resulted in fluorescence efficiencies (calculated as fluorescence peak area/absorbance peak area) that were approximately 12-fold and 4-fold greater for the oxoA2E compounds identified as peaks 1 and 3, respectively, as compared to A2E. For peak 3, selected ion monitoring revealed *m*/*z* 608 indicative of the addition of one oxygen atom (+16) at a carbon-carbon double bond while peak 1 exhibited *m*/*z* 624 indicative of the addition of 2 oxygen atoms. From our previous work,[34] we can assume that the corresponding oxygen-containing moieties were a furan and endoperoxide. On the other hand, photooxidation of A2E within the long arm of the molecule (Fig. 5: peak 2) reduced or negated fluorescence when excited at 430 nm. This change would occur because the hypsochromic shift (blue-shift) associated with loss of a carbon-carbon double bond on the long arm of A2E, displaces the excitation maxima away from the 488 nm-wavelength utilized by fundus autofluorescence imaging.

Fundus autofluorescence emanating from photoreceptor cell outer segments

Bisretinoid lipofuscin compounds form in photoreceptor cells and are subsequently deposited in RPE due to daily shedding of outer segments by photoreceptor cells and uptake of the debris by RPE phagocytosis.[35] Consequently in a healthy retina, the bisretinoids of the lipofuscin synthetic pathway are present at minimal levels in the photoreceptor cells. However, when photoreceptor cells are compromised, such as occurs in association with failure of RPE cells to phagocytose,[33] photoreceptor outer segments become an abnormal but intense source of fundus autofluorescence.

At least some of the lipofuscin-associated pigments that form in photoreceptor cell outer segments include A2-DHPPE, all-*trans*-retinal dimer, all-*trans*-retinal dimer-PE and A2PE. The phosphatidyl-pyridinium pigment A2PE (excitation maximum ~449 nm) forms in photoreceptor cell outer segments from reactions of all-*trans*-retinal with the phospholipid,

phosphatidylethanolamine.[8,27,36,37] Amongst the group of bisretinoids mentioned above, A2PE of the A2E biosynthetic pathway is distinguished by the ease with which it undergoes phosphate hydrolysis in RPE cell lysosomes resulting in cleavage of A2PE and release of A2E.[27,38] Consequently A2PE is not detected in RPE and can thus be used as a marker of bisretinoid residency in outer segments.

Thus using A2PE as an example, we sought to understand contributions to fundus autofluorescence from bisretinoids in photoreceptor cells. To this end we compared the fluorescence emission of A2PE and A2E in PBS with 2% DMSO and in two organic solvents, methanol and chloroform, the latter being the more hydrophobic of the two (Fig. 2). Like A2E, A2PE exhibited a redshift in emission maxima when excited at the longer wavelength (430 nm *versus* 488 nm) in both methanol and chloroform; this redshift was not observed with PBS/DMSO. Solvent dependency of the A2PE emission maximum was also observed. The fluorescence intensity of A2PE was similar in PBS/DMSO and chloroform but the difference in fluorescence intensity between A2E and A2PE was most pronounced in PBS/DMSO with emission of A2PEbeing ~4-fold greater. The dual character of the PBS/DMSO mixture would allow DMSO to solvate the hydrophobic arms of A2E and A2PE while the hydrophilic side-arms of A2E would interact with the water molecules; thus this system probably best mimics the cellular milieu. The fluorescence efficiency of A2PE at 488 nm excitation was also found to be more pronounced than A2E when both compounds were injected into the HPLC and monitored for absorbance and fluorescence (Fig. 6). Specifically, the fluorescence efficiency of A2PE was 1.8-fold greater than A2E (A2E: 20,069; A2PE: 36,103). The more pronounced fluorescence of A2PE may reflect, in part, an excitation maximum (~449 nm) that is closer to 488 nm than is the excitation maximum of A2E (~439 nm).

Another factor that may potentiate the contribution of A2PE to fundus hyperautofluorescence is photooxidation. Like A2E, A2PE and the other bisretinoid precursors are photoreactive compounds that upon photon absorbance can generate reactive forms of oxygen.[34,39-41] Also like A2E (Fig. 5), A2PE undergoes photooxidation. Shown in Fig. 7 are chromatographic (Fig. 7A, B) and mass spectrometric (Fig. 7C, D) analysis of 430 nm-irradiated samples of synthesized A2PE. Because of increased polarity, the multiple peaks attributable to photooxidized forms of A2PE elute ahead of the parent A2PE compound (Fig. 7A). Examination of irradiated samples of A2PE (Fig. 7A, B; black traces) also revealed that some of these photooxo-A2PE species exhibit substantial increases in fluorescence efficiency, since their fluorescence peak heights (Fig. 7B) were considerably increased relative to absorbance peak heights (Fig. 7A). Photooxidation of the sample is evidenced from the mass spectrometry profile: in addition to the *m*/*z* of 1223 attributable to A2PE (synthesized from dipalmitoyl-phosphatidylethanolamine), a series of higher *m*/*z* peaks appear at successive increments of mass 16 (the mass of oxygen).

Autofluorescence and retinoids

In addition to heightened autofluorescence in parafoveal rings and in the surround of geographic atrophy, hyperautofluorescence associated with retinal disease can take the form of diffuse puncta that on color fundus photographs present as scattered white dots.[42] These

lesions are typical of at least two autosomal recessive disorders: fundus albipunctatus due to mutations in *RDH5*, the gene that encodes 11-*cis*-retinol dehydrogenase,[43] and punctata albescens, most frequently associated with the *RLBP1* gene for cellular retinaldehyde-binding protein (CRALBP).[44] Since both of the affected proteins contribute to the regeneration of 11-*cis*-retinal *via* the retinoid cycle, it is of interest to consider whether autofluorescence in these disorders reflects accumulations of retinoid.[42]

To begin to address this question, we measured the spectra of two of the retinoids of the visual cycle. With all-*trans*-retinyl palmitate (60 μM), we observed a fluorescence peak at 476 nm in methanol and 505 nm in PBS (with 2% DMSO) with excitation at 380 nm (Fig. 8). However, no fluorescence was noted with excitations at 430 nm or 488 nm in either solvent (not shown). Lack of a contribution of retinyl ester to fundus autofluorescence would be consistent with the finding in RPE65-related disease that retinyl esters accumulate in abundance in RPE cells,[45] while at the same time, fundus autofluorescence is absent.[12]

When all-*trans*-retinal was placed in methanol (60 μM), we observed a fluorescence that peaked at 535 nm with 380 nm excitation and peak emission at 570 nm with excitation at 430 nm (Fig. 8). Fluorescence was not observed with an excitation at 488 nm in methanol (Fig. 8F). In PBS/DMSO with 380 nm excitation, all-*trans*-retinal fluorescence was essentially absent at a concentration of 60 μM, but weak fluorescence was observed at a concentration of 120 μM (Fig. 8H, I). With excitation at 430 and 488 nm and at concentrations of both 60 and 120 μM, all-*trans*-retinal fluorescence was absent (Fig. 8K, L, N, O). Recordings from solvent only are presented for comparison (Fig. 8F, G, J, M).

It is worth noting that the issue of whether all-*trans*-retinal exhibits fluorescence has been notoriously difficult to resolve; this is in part because the fluorescence excitation spectra observed have not corresponded to the absorption spectra and a strong concentration dependence indicates that fluorescence is associated with molecular interactions between molecules of all-*trans*-retinal.[46, 47] Additionally, a contribution to fundus autofluorescence from all-*trans*-retinal in photoreceptor cells would presuppose that all-*trans*-retinal is released in a free state after it forms following photoisomerization of 11-*cis*-retinal. But all-*trans*-retinal is a toxic aldehyde-bearing compound[48] and experiments indicate that mechanisms[49, 50] are available to chaperone all-*trans*-retinal until it is reduced to all-*trans*-retinol, thereby minimizing the opportunity for free all-*trans*-retinal to exist.[51] Taken together, the spectral data presented here do not support the notion that fluorescent puncta observed in fundus autofluorescent images originate from all-*trans*-retinal.

Conclusions

The fundus autofluorescence that can be imaged in a healthy retina derives primarily from RPE bisretinoid chromophores. Emission spectra obtained from the full complement of RPE lipofuscin material present in histological sections of human retina, reflect fluorescence from a complicated mixture of bisretinoid fluorophores that vary with respect to excitation and emission spectra and fluorescence efficiency. Added to this complexity is the solvatochromism exhibited by the lipofuscin bisretinoids along with hypsochromic shifts in spectral profiles and changes in fluorescence efficiency that accompany photooxidation of

these pigments. Retinyl esters and all-*trans*-retinal, two retinoids of the visual cycle, do not exhibit spectral features consistent with a contribution to fundus autofluorescence.

Clinically noted increases in fundus autofluorescence, such as occurs in recessive Stargardt disease, can represent disease-related augmentation of lipofuscin within RPE cells. It is frequently supposed that accelerated phagocytosis of photoreceptor outer segment membrane can also intensify lipofuscin levels in RPE. However, the bisretinoids of retinal lipofuscin form in photoreceptor cell outer segments prior to disc shedding and phagocytosis and not in the phagosome or RPE lysosome. Thus, the production of this material depends on the availability of precursors inphotoreceptor cells,[51] but is unlikely to be determined by the rate at which outer segment membrane is cleared by RPE.

In summary, the contributions that the various bisretinoid species make to fundus autofluorescence is determined by their excitation and emission spectra and is related to abundance, fluorescence efficiency and the extent to which the bisretinoid pigments become photooxidized. It is often assumed that fundus autofluorescence is derived only from bisretinoids that have been deposited in RPE cells as lipofuscin; however conditions may exist wherein aberrant autofluorescence can also originate from the bisretinoid precursors located in photoreceptor cell outer segments.[33] Understanding the source and reasons for fundus hyperautofluorescence is essential to efforts aimed at using fundus autofluorescence imaging to evaluate progression of retinal disease and to appraise the effectiveness of treatments as they become available.

Acknowledgments

This work was supported by National Institutes of Health Grant EY 12951, the Kaplen Foundation (JRS), a grant from Research to Prevent Blindness to the Department of Ophthalmology and a post-doctoral fellowship from National Research Foundation of Korea (KDY).

References

1. von Ruckmann A, Fitzke FW, Bird AC. Distribution of fundus autofluorescence with a scanning laser ophthalmoscope. Br. J. Ophthalmol. 1995; 79:407–412. [PubMed: 7612549]
2. Spaide, RF. Atlas of Fundus Autofluorescence Imaging. Holz, FG.; Schmitz-Valckenberg, S.; Spaide, RF.; Bird, AC., editors. Springer-Verlag; Berlin, Heidelberg: 2007. p. 49-54.
3. Delori FC. Spectrophotometer for noninvasive measurement of intrinsic fluorescence and reflectance of the ocular fundus. Appl. Opt. 1994; 33:7439–7452. [PubMed: 20941307]
4. Morgan JI, Hunter JJ, Masella B, Wolfe R, Gray DC, Merigan WH, Delori FC, Williams DR. Light-induced retinal changes observed with high-resolution autofluorescence imaging of the retinal pigment epithelium. Invest. Ophthalmol. Visual Sci. 2008; 49:3715–3729. [PubMed: 18408191]
5. Delori FC, Dorey CK, Staurenghi G, Arend O, Goger DG, Weiter JJ. In vivo fluorescence of the ocular fundus exhibits retinal pigment epithelium lipofuscin characteristics. Invest. Ophthalmol. Visual Sci. 1995; 36:718–729. [PubMed: 7890502]
6. von Ruckmann A, Fitzke FW, Bird AC. In vivo fundus autofluorescence in macular dystrophies. Arch. Ophthalmol. 1997; 115:609–615. [PubMed: 9152128]
7. Delori FC, Goger DG, Dorey CK. Age-related accumulation and spatial distribution of lipofuscin in RPE of normal subjects. Invest. Ophthalmol. Visual Sci. 2001; 42:1855–1866. [PubMed: 11431454]
8. Parish CA, Hashimoto M, Nakanishi K, Dillon J, Sparrow JR. Isolation and one-step preparation of A2E and iso-A2E, fluorophores from human retinal pigment epithelium. Proc. Natl. Acad. Sci. U. S. A. 1998; 95:14609–14613. [PubMed: 9843937]

9. Fishkin N, Sparrow JR, Allikmets R, Nakanishi K. Isolation and characterization of a retinal pigment epithelial cell fluorophore: an all-trans-retinal dimer conjugate. Proc. Natl. Acad. Sci. U. S. A. 2005; 102:7091–7096. [PubMed: 15870200]
10. Kim SR, Jang YP, Jockusch S, Fishkin NE, Turro NJ, Sparrow JR. The all-trans-retinal dimer series of lipofuscin pigments in retinal pigment epithelial cells in a recessive Stargardt disease model. Proc. Natl. Acad. Sci. U. S. A. 2007; 104:19273–19278. [PubMed: 18048333]
11. Wu Y, Fishkin NE, Pande A, Pande J, Sparrow JR. Novel lipofuscin bisretinoids prominent in human retina and in a model of recessive Stargardt disease. J. Biol. Chem. 2009; 284:20155–20166. [PubMed: 19478335]
12. Lorenz B, Wabbels B, Wegscheider E, Hamel CP, Drexler W, Presing MN. Lack of fundus autofluorescence to 488 nanometers from childhood on in patients with early-onset severe retinal dystrophy associated with mutations in RPE65. Ophthalmology. 2004; 111:1585–1594. [PubMed: 15288992]
13. Eagle RC, Lucier AC, Bernardino VB, Yanoff M. Retinal pigment epithelial abnormalities in fundus flavimaculatus. Ophthalmology. 1980; 87:1189–1200. [PubMed: 6165950]
14. Weng J, Mata NL, Azarian SM, Tzekov RT, Birch DG, Travis GH. Insights into the function of Rim protein in photoreceptors and etiology of Stargardt's disease from the phenotype in abcr knockout mice. Cell. 1999; 98:13–23. [PubMed: 10412977]
15. Kim SR, Fishkin N, Kong J, Nakanishi K, Allikmets R, Sparrow JR. The Rpe65 Leu 450 Met variant is associated with reduced levels of the RPE lipofuscin fluorophores A2E and iso-A2E. Proc. Natl. Acad. Sci. U. S. A. 2004; 101:11668–11672. [PubMed: 15277666]
16. Delori FC, Staurenghi G, Arend O, Dorey CK, Goger DG, Weiter JJ. In vivo measurement of lipofuscin in Stargardt's disease-Fundus flavimaculatus. Invest. Ophthalmol. Visual Sci. 1995; 36:2327–2331. [PubMed: 7558729]
17. Lois N, Holder GE, Bunce CV, Fitzke FW, Bird AC. Phenotypic subtypes of Stargardt macular dystrophy-fundus flavimaculatus. Arch. Ophthalmol. 2001; 119:359–369. [PubMed: 11231769]
18. Vasireddy V, Jablonski MM, Khan NW, Wang XF, Sahu P, Sparrow JR, Ayyagari R. Elovl4 5-bp deletion knock-in mouse model for Stargardt-like macular degeneration demonstrates accumulation of ELOVL4 and lipofusin. Exp. Eye Res. 2009; 89:905–912. [PubMed: 19682985]
19. Chung JE, Spaide RF. Fundus autofluorescence and vitelliform macular dystrophy. Arch. Ophthalmol. 2004; 122:1078. [PubMed: 15249383]
20. Wing GL, Blanchard GC, Weiter JJ. The topography and age relationship of lipofuscin concentration in the retinal pigment epithelium. Invest. Ophthalmol. Visual Sci. 1978; 17:601–607. [PubMed: 669891]
21. Young RW. Pathophysiology of age-related macular degeneration. Surv. Ophthalmol. 1987; 31:291–306. [PubMed: 3299827]
22. Zhou J, Jang YP, Kim SR, Sparrow JR. Complement activation by photooxidation products of A2E, a lipofuscin constituent of the retinal pigment epithelium. Proc. Natl. Acad. Sci. U. S. A. 2006; 103:16182–16187. [PubMed: 17060630]
23. Zhou J, Kim SR, Westlund BS, Sparrow JR. Complement activation by bisretinoid constituents of RPE lipofuscin. Invest. Ophthalmol. Visual Sci. 2009; 50:1392–1399. [PubMed: 19029031]
24. Holz FG, Bellman C, Staudt S, Schutt F, Volcker HE. Fundus autofluorescence and development of geographic atrophy in age-related macular degeneration. Invest. Ophthalmol. Visual Sci. 2001; 42:1051–1056. [PubMed: 11274085]
25. Robson AG, Michaelides M, Saihan Z, Bird AC, Webster AR, Moore AT, Fitzke FW, Holder GE. Functional characteristics of patients with retinal dystrophy that manifest abnormal parafoveal annuli of high density fundus autofluorescence: a review and update. Doc. Ophthalmol. 2008; 116:79–89. [PubMed: 17985165]
26. Schmitz-Valckenberg S, Jorzik J, Unnebrink K, Holz FG. Analysis of digital scanning laser ophthalmoscopy fundus autofluorescenceimages of geographic atrophy in advanced age-related macular degeneration. Graefe's Arch. Clin. Exp. Ophthalmol. 2002; 240:73–78. [PubMed: 11933894]

27. Liu J, Itagaki Y, Ben-Shabat S, Nakanishi K, Sparrow JR. The biosynthesis of A2E, a fluorophore of aging retina, involves the formation of the precursor, A2-PE, in the photoreceptor outer segment membrane. J. Biol. Chem. 2000; 275:29354–29360. [PubMed: 10887199]
28. Sakai N, Decatur J, Nakanishi K, Eldred GE. Ocular age pigment "A2E": An unprecedented pyridinium bisretinoid. J. Am. Chem. Soc. 1996; 118:1559–1560.
29. Fishkin N, Pescitelli G, Sparrow JR, Nakanishi K, Berova N. Absolute configurational determination of an all-*trans*-retinal dimer isolated from photoreceptor outer segments. Chirality. 2004; 16:637–641. [PubMed: 15382205]
30. Delori, FC.; Keilhauer, C.; Sparrow, JR.; Staurenghi, G. Atlas of Fundus Autofluorescence Imaging. Holz, FG.; Schmitz-Valckenberg, S.; Spaide, RF.; Bird, AC., editors. Springer-Verlag; Berlin, Heidelberg: 2007. p. 17-29.
31. Sparrow JR, Parish CA, Hashimoto M, Nakanishi K. A2E, a lipofuscin fluorophore, in human retinal pigmented epithelial cells in culture. Invest. Ophthalmol. Visual Sci. 1999; 40:2988–2995. [PubMed: 10549662]
32. Kim SR, Jang Y, Sparrow JR. Photooxidation of RPE Lipofuscin bisretinoids enhanced fluorescence intensity. Vision Res. 2010; 50:729–736. [PubMed: 19800359]
33. Sparrow JR, Yoon K, Wu Y, Yamamoto K. Interpretations of fundus autofluorescence from studies of the bisretinoids of retina. Invest. Ophthalmol. Visual Sci. 2010; 51:4351–4357. [PubMed: 20805567]
34. Jang YP, Matsuda H, Itagaki Y, Nakanishi K, Sparrow JR. Characterization of peroxy-A2E and furan-A2E photooxidation products and detection in human and mouse retinal pigment epithelial cells lipofuscin. J. Biol. Chem. 2005; 280:39732–39739. [PubMed: 16186115]
35. Bok D. Retinal photoreceptor-pigment epithelium interactions. Friedenwald lecture. Invest. Ophthalmol. Visual Sci. 1985; 26:1659–1694. [PubMed: 2933359]
36. Ben-Shabat S, Parish CA, Vollmer HR, Itagaki Y, Fishkin N, Nakanishi K, Sparrow JR. Biosynthetic studies of A2E, a major fluorophore of RPE lipofuscin. J. Biol. Chem. 2002; 277:7183–7190. [PubMed: 11756445]
37. Kim SR, He J, Yanase E, Jang YP, Berova N, Sparrow JR, Nakanishi K. Characterization of dihydro-A2PE: an Intermediate in the A2E biosynthetic pathway. Biochemistry. 2007; 46:10122–10129. [PubMed: 17685561]
38. Sparrow JR, Kim SR, Cuervo AM, Bandhyopadhyayand U. A2E, a pigment of RPE lipofuscin is generated from the precursor A2PE by a lysosomal enzyme activity. Adv. Exp. Med. Biol. 2008; 613:393–398. [PubMed: 18188969]
39. Ben-Shabat S, Itagaki Y, Jockusch S, Sparrow JR, Turro NJ, Nakanishi K. Formation of a nona-oxirane from A2E, alipofuscin fluorophore related to macular degeneration, and evidence of singlet oxygen involvement. Angew. Chem., Int. Ed. 2002; 41:814–817.
40. Kim SR, Jockusch S, Itagaki Y, Turro NJ, Sparrow JR. Mechanisms involved in A2E oxidation. Exp. Eye Res. 2008; 86:975–982. [PubMed: 18439997]
41. Sparrow JR, Zhou J, Ben-Shabat S, Vollmer H, Itagaki Y, Nakanishi K. Involvement of oxidative mechanisms in blue light induced damage to A2E-laden RPE. Invest. Ophthalmol. Visual Sci. 2002; 43:1222–1227. [PubMed: 11923269]
42. Genead MA, Fishman GA, Lindeman M. Spectral-domain optical coherence tomography and fundus autofluorescence characteristics in patients with fundus albipunctatus and retinitis punctata albescens. Ophthalmic Genet. 2010; 31:66–72. [PubMed: 20450307]
43. Yamamoto H, Yakushijin K, Kusuhara S, Escano MF, Nagai A, Negi A. A novel RDH5 gene mutation in a patient with fundus albipunctatus presenting with macular atrophy and fading white dots. Am. J. Ophthalmol. 2003; 136:572–574. [PubMed: 12967826]
44. Humbert G, Delettre C, Sénéchal A, Bazalgette C, Barakat A, Bazalgette C, Arnaud B, Lenaers G, Hamel CP. Homozygous deletion related to Alu repeats in RLBP1 causes retinitis punctata albescens. Invest. Ophthalmol. Visual Sci. 2006; 47:4719–4724. [PubMed: 17065479]
45. Redmond TM, Yu S, Lee E, Bok D, Hamasaki D, Chen N, Goletz P, Ma J-X, Crouch RK, Pfeifer K. Rpe65 is necessary for production of 11-cis-vitamin A in the retinal visual cycle. Nat. Genet. 1998; 20:344–351. [PubMed: 9843205]

46. Alex S, Thanh HL, Vocelle D. Studies of the effect of hydrogen bonding on the absorption and fluorescence spectra of all-trans-retinal at room temperature. Can. J. Chem. 1992; 70:880–887.

47. Takemura T, Hug G, Das PK, Becker RS. Visual pigments. 9 Fluorescence of dimers of retinals. J. Am. Chem. Soc. 1978; 100:2631–2634.

48. Maeda A, Maeda T, Golczak M, Chou S, Desai A, Hoppel CL, Matsuyama S, Palczewski K. Involvement of all-trans-retinal in acute light-induced retinopathy of mice. J. Biol. Chem. 2009; 284:15173–15183. [PubMed: 19304658]

49. Schadel SA, Heck M, Maretzki D, Filipek S, Teller DC, Palczewski K, Hofmann KP. Ligand channeling with a G-protein-coupled receptor: The entry and exit of retinal in native opsin. J. Biol. Chem. 2003; 278:24896–24903. [PubMed: 12707280]

50. Anderson RE, Maude MB. Phospholipids of bovine outer segments. Biochemistry. 1970; 9:3624–3628. [PubMed: 5509846]

51. Sparrow JR, Wu Y, Kim CY, Zhou J. Phospholipid meets all-*trans*-retinal: the making of RPE bisretinoids. J. Lipid Res. 2010; 51:247–261. [PubMed: 19666736]

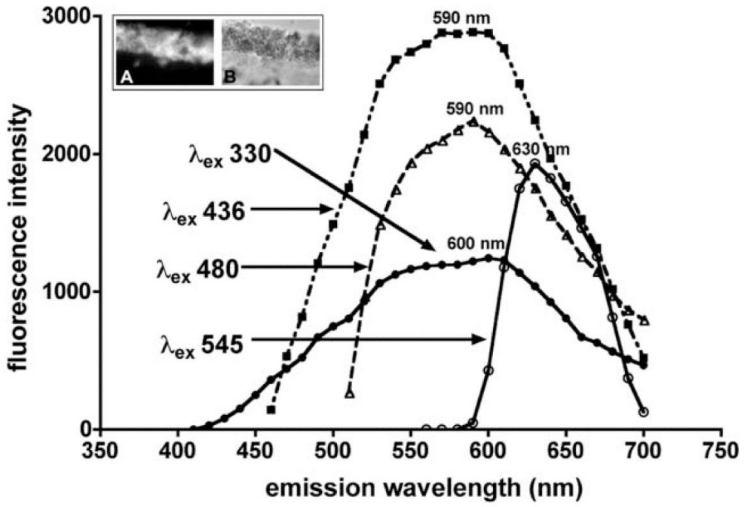

Fig. 1.

Fluorescence emission spectra of whole lipofuscin in human RPE. Measurements were taken using fluorescence microscopy, cryostat sections of the eye and a range of excitation wavelengths (λ_{ex}). Inset above: fluorescence (A) and phase contrast (B) images of a representative area of RPE monolayer. Emission maxima are presented in nanometres (nm).

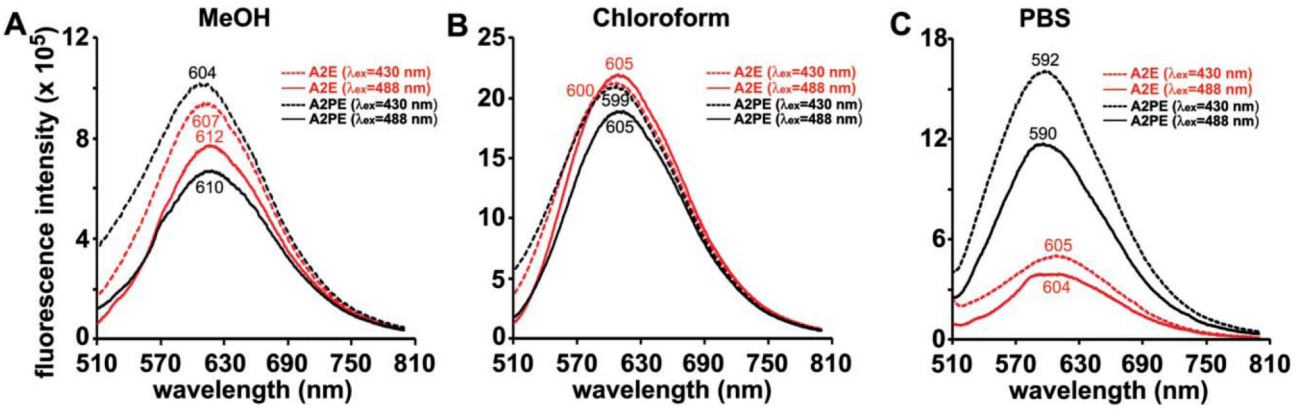

Fig. 2.

Emission spectra of A2E and A2PE in methanol (MeOH) (A) and chloroform (B) and phosphate buffered saline (PBS) with 2% DMSO (C). Bandpass slit was 6 nm. Emission was recorded with an excitation of 430 or 488 nm. The final concentration of each compound in solvent was 30 μM. The unit of fluorescence intensity is counts per second. Emission maxima (nm) are indicated.

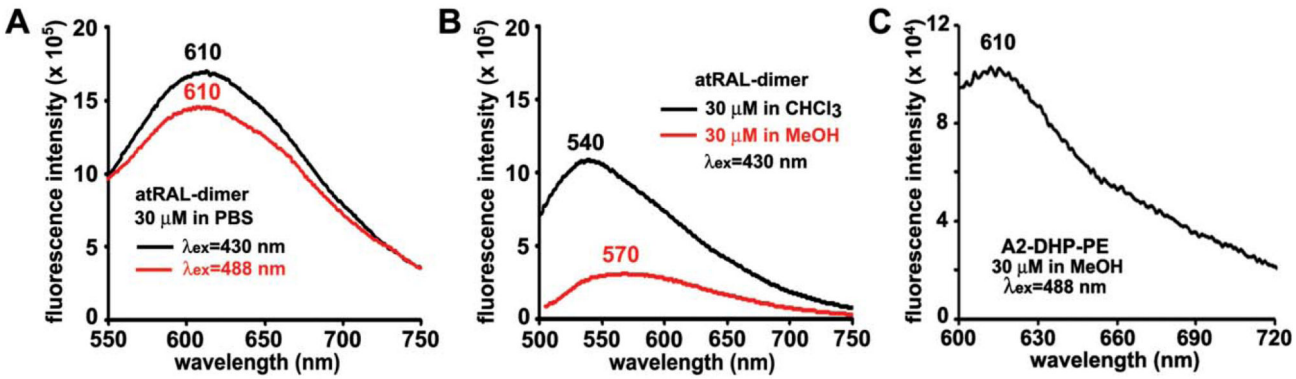

Fig. 3.

Fluorescence emission spectra of the bisretinoid lipofuscin pigments all-*trans*-retinal dimer (A, B) and A2-DHP-PE (C) in PBS, chloroform ($CHCl_3$) and/or methanol (MeOH). The final concentration of the compounds was 30 μM and the excitation wavelength (λ_{ex}) was 430 or 488 nm. Unit of fluorescence intensity is counts per second. Emission maxima are presented (nm). Bandpass slit was set at 8 nm for A2-DHP-PE and 6 nm for all-*trans*-retinal dimer.

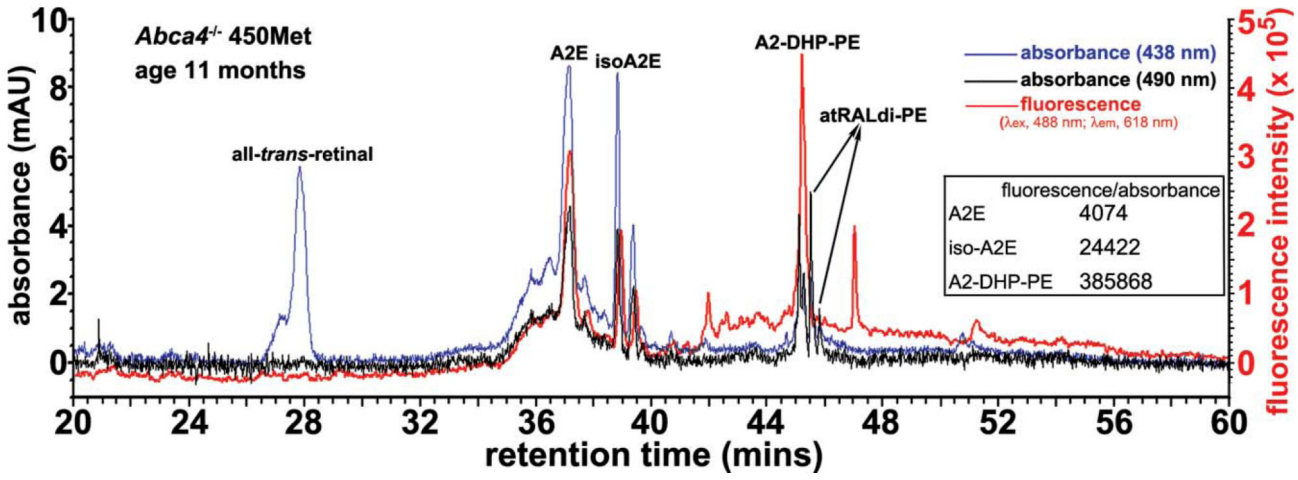

Fig. 4.

Bisretinoids of retina exhibit differences in fluorescence efficiency. Reverse phase HPLC (C18 column). Injectant was a hydrophobic extract of eyes from *Abca4*$^{-/-}$ mice (age 11 months; homozygous for methionine at the Rpe65 450 variant) with absorbance (438 and 490 nm) and fluorescence [excitation (λ_{ex}), 488 nm; emission (λ_{em}), 618 nm] monitoring. mAU, milliabsorbance units; fluorescence intensity in arbitrary units. Inset: table of fluorescence efficiency (λ_{ex} 488 nm) for A2E, isoA2E and A2-DHP-PE.

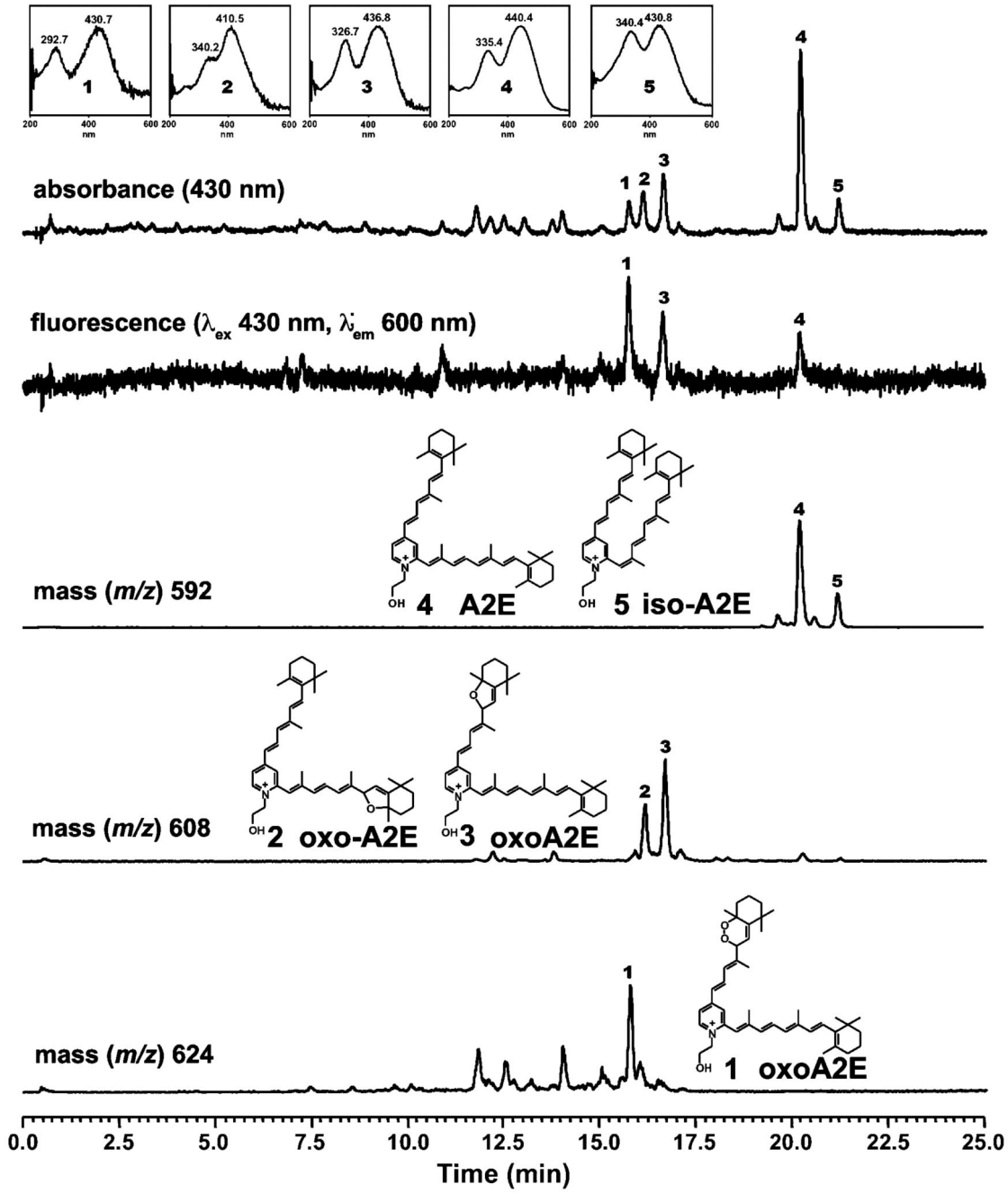

Fig. 5.

Fluorescence efficiency of the RPE lipofuscin bisretinoid A2E is increased following photooxidation on the short arm of the molecule. Samples of A2E were irradiated at 430 nm (2 min) to generate photooxidation products (oxo-A2E 1, 2, 3). Analysis by reversed phase UPLC with monitoring of absorbance (430 nm), fluorescence (λ_{ex} 430 nm; λ_{em} 600 nm) and selected ion monitoring at mass to charge ratio (*m*/*z*) 592, 608 and 624. Fluorescence efficiency was 1.28 for di-oxo-A2E (peak 1); 0.45 for monooxo-A2E (peak 3) and 0.1 for A2E (peak 4).

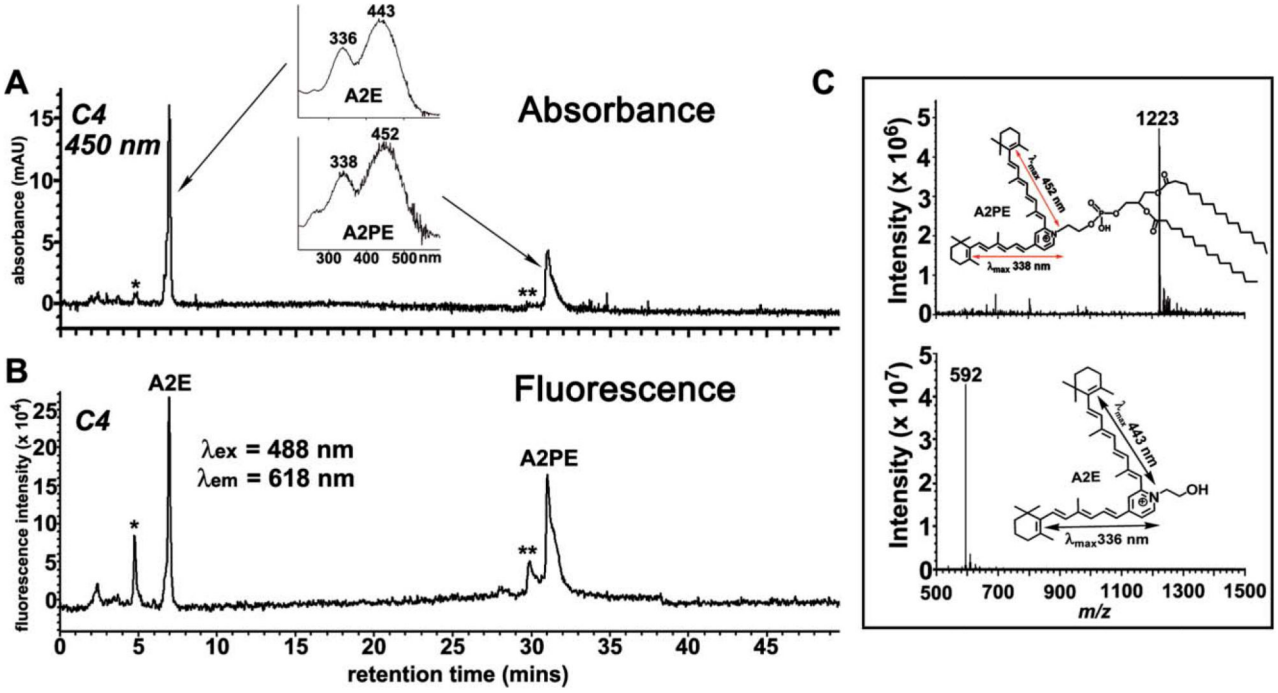

Fig. 6.

At an excitation of 488 nm the fluorescence emission of A2PE is greater than A2E. The analyte was a 1: 1 mixture of A2E and A2PE, each at 30 μM in PBS with 0.6% DMSO. Reverse phase HPLC (C4 column) with detection of absorbance (A) by photodiode array (450 nm) and fluorescence (B) with multi λ fluorescence detector (excitation, 488 nm; emission, 618 nm; bandwidth, 18 nm). Insets in A: UV-visible absorbance spectra of A2E and A2PE. *, oxidized A2E; **, oxidized A2PE. (C) Mass spectrometric analysis and planar structures (insets) of the two chromatographic peaks in A and B, corresponding to A2PE (top) and A2E (bottom). (↔), electronic transition assignments.

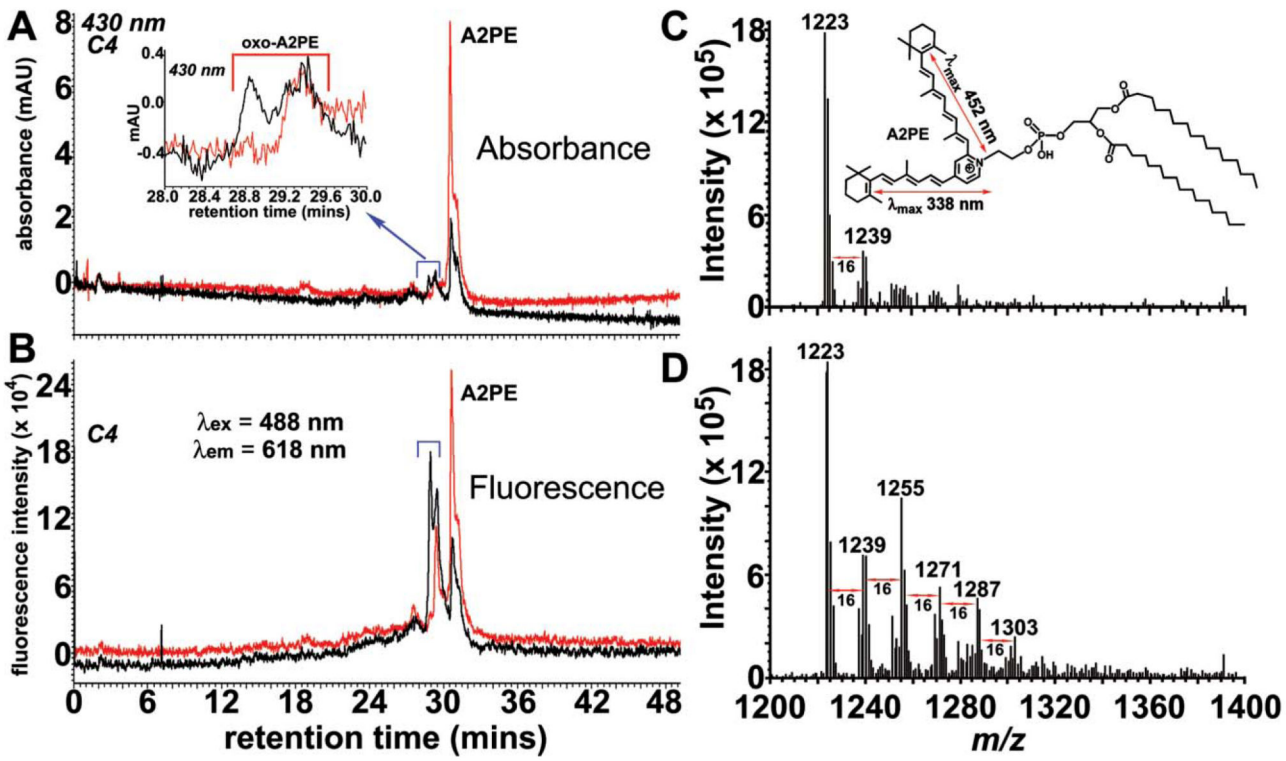

Fig. 7.

Photooxidation of A2PE. A2PE (200 μM) in PBS with 2% DMSO was irradiated for 30 min at 430 nm. Representative reverse phase HPLC chromatograms (C4 column) with monitoring of absorbance and (A) and fluorescence (B) at indicated wavelengths. Inset in A: expanded chromatogram between retention time 28-30 min. ESI-MS spectrometry of unirradiated (C) and irradiated (D) A2PE. Inset in C: structure and electronic transition assignments (↔) of A2PE. The molecular ion peak at mass-to-charge (*m*/*z*) ratio 1223 corresponds to molecular mass of A2PE synthesized from dipalmitoyl-phosphatidylethanolamine (DP-PE). Peaks differing in *m*/*z* by 16 (*e.g.* 1239, 1255, 1271 *etc*.) are indicative of A2PE photooxidation.

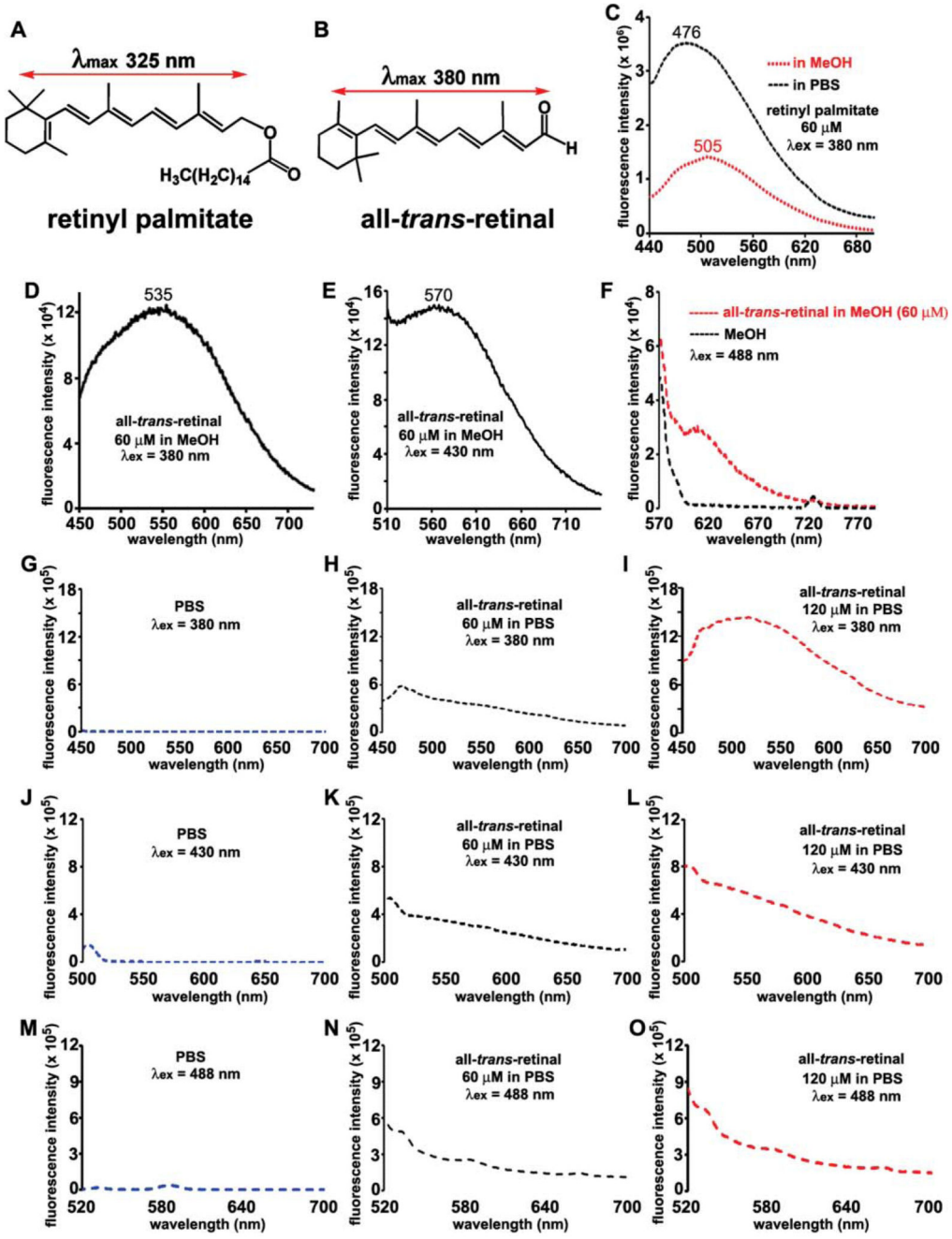

Fig. 8.

Fluorescence emission spectra of retinyl palmitate and all-*trans*-retinal. Structures and electronic transition assignments () for retinyl palmitate (A) and all-*trans*-retinal (B). Emission of retinyl palmitate (C) and all-*trans*-retinal (D-F, H, I, K, L, N, O) recorded in methanol (MeOH) ↔ and phosphate buffered saline (PBS), both with 0.6-1.2% DMSO; excitation wavelengths (λ_{ex}) and concentrations (μM) are indicated. Recordings with MeOH (F) or PBS (G, J, M) alone are also presented. Bandpass slit: 6 nm for retinyl palmitate and

all-*trans*-retinal in MeOH (λ_{ex} 380 nm) and in PBS; 10 nm for all-*trans*-retinal (in MeOH λ_{ex} 430 nm).